https://doi.org/10.20965/jrm.2022.p0373

Paper:

Development of a Spiral Shaped Soft Holding Actuator Using Extension Type Flexible Pneumatic Actuators

So Shimooka*, Tetsuya Akagi, Shujiro Dohta**, Takashi Shinohara***, and Takumi Kobayashi****

*Graduate School of Natural Science and Technology, Okayama University
3-1-1 Tsushima-naka, Kita-ku, Okayama 700-8530, Japan
E-mail: shimooka@okayama-u.ac.jp
**Department of Intelligent Mechanical Engineering, Okayama University of Science
1-1 Ridai-cho, Kita-ku, Okayama 700-0005, Japan
E-mail: {akagi@are, dohta@are}.ous.ac.jp, t20rm02kt@ous.jp
***Design and Manufacturing Center, Organization for Research Development and Outreach, Okayama University of Science
1-1 Ridai-cho, Kita-ku, Okayama 700-0005, Japan
E-mail: shinohara@pub.ous.ac.jp
[Received September 16, 2021; accepted March 4, 2022]

Recently, several pneumatic soft actuators have been applied to wearable and welfare devices to provide nursing care and physical support for the elderly and disabled. In this study, as a wearable soft actuator for holding body, a spiral shaped soft holding actuator that can wrap a user according to their body shape was proposed and tested. The construction and operating principle of the tested soft actuator with circumferential restraint mechanism using three extension type flexible pneumatic actuators (EFPAs) has been discussed. As a result, it was found that the tested actuator could hold elbows and knees when the joint is in motion. An analytical model of the spiral actuator was also proposed to achieve an optimal design. It can be confirmed that the proposed analytical model can predict the shape of the actuator when various EFPAs are pressurized.

Keywords: spiral shaped soft holding actuator, extension type flexible pneumatic actuator, circumference restraint mechanism, analytical model

1. Introduction

Recently, the rapid increase in the elderly population and reduction in birth rates in Japan have been a serious concern. The proportion of elderly became more than 28.9% in 2020 [a]. The ratio will be expected to reach 35.3% by 2040. Consequently, various wearable pneumatic equipments to support nursing care and welfare assistance provided to the elderly and disabled people using pneumatic soft actuators have been actively researched and developed [1–8]. The soft actuators used in such equipment must have superior human-friendly properties. A pneumatic actuator that has a higher force/weight ratio and compliance owing to air compressibility is promising. The user would not be injured and would be less burden by the advantages of pneumatic soft actuators. From a welfare assistance standpoint, the most difficult task is transferring the bedridden elderly people. During transfer, a caregiver should lift the elderly without hurt. The caregiver provides lifting and holding force to the elderly by increasing the contact area between them to distribute the lifting force. To realize a supporting device for transferring patients, it is necessary to develop a holding device that can support the elderly while the holding force is distributed over a large contact area.

Therefore, in this study, we aim to develop a soft actuator that can easily wrap the human body and release it. We think that the pneumatic type wrapping actuator has advantages in reducing the care time and maintaining safety based on the backdrivability. It is better that the required actuator can connect to anywhere in the body, such as joints. From a quality of life (QOL) standpoint, it is ideal to develop a holding actuator such that the holding joint can move even if the actuator completely wraps the joint. Therefore, based on the features of the required actuator, it is not necessary for the user to fix a supporter such as a cloth or band. The device using a cloth and band requires safety equipment because of the possibility of an accident. However, the proposed actuator and pneumatic system have safety functions owing to their compressibility and flexibility. Therefore, the proposed actuator comes off and buckles more than a certain pulling and wrapping force. In addition, it seems necessary that the wrapping pressure of the proposed actuator is lower than that of the typical pressure (maximum is approximately 200 mmHg) used by a blood pressure monitor (sphygmo-manometer) to prevent the blood congestion [b]. If such an actuator can be developed, it can also massage the joint, which includes many muscle tendons.

A spiral-shaped soft actuator is useful for holding objects softly by distributing the holding force over a large contact area. Therefore, various spiral-shaped actuators using soft mechanisms have been developed [9–12]. In this study, a spiral soft-shaped actuator using extension-

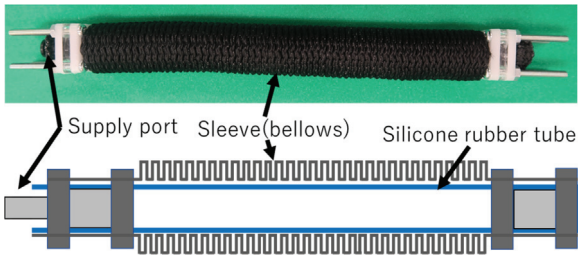

Fig. 1. Overview and schematic of EFPA [13].

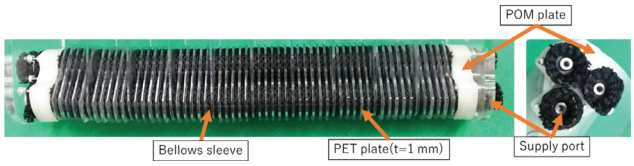

Fig. 2. Construction of reinforced EFPA with circumferential restrains.

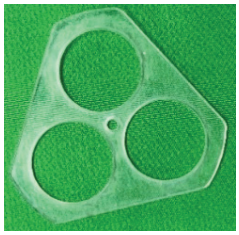

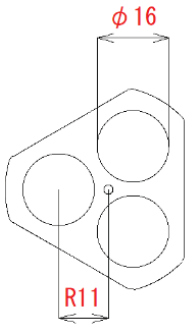

Fig. 3. Shape of restraint PET plates ($t = 1$ mm).

type flexible pneumatic actuators (EFPAs) with reinforced circumference restraints is proposed and tested as a holding actuator for moving the elbow and knee joints. The construction and operating principles of the tested spiral-shaped actuator are described. In addition, to realize a wearable device that considers the wrapping pressure and force, we propose a simple analytical model that can predict the shape of the actuator by varying the displacement of each EFPA in this paper.

2. Extension Type Flexible Pneumatic Actuator

Figure 1 demonstrates the overview and schematic diagram of EFPA [13–16], which is used as a soft actuator in the proposed spiral-shaped actuator. The actuator consists of a silicone rubber tube covered with a bellows-type nylon sleeve (Swiftrans Co. Ltd., Stretching hose). The rubber tube in the sleeve has an inner diameter of 8 mm and outer diameter of 11 mm. The EFPA can extend approximately 2.5 times its original length when it is pressurized to 500 kPa. The maximum pulling force provided by the EFPA with an original length of 200 mm is approximately 60 N. The pulling force depends on the elastic properties of the rubber tube, such as its material and thickness. The operating principle of the EFPA is as follows. When the EFPA is pressurized, the inner silicone rubber tube expands in both the circumferential and axial directions. However, the EFPA extends only toward the axial direction because the bellows-shaped nylon sleeve restricts the extension in the circumferential direction. When the EFPA is decompressed, it returns to its original length because of the restoring force of the inner rubber tube. The EFPA is suitable as a soft actuator of the proposed spiral actuator because of its flexibility and lightness. However, it is difficult to maintain the specific shape of the EFPA because of its flexibility. Therefore, the reinforced restraint mechanism is required to maintain the spiral shape.

Figure 2 shows how the reinforced EFPA with circumferential restraints is constructed [15, 16]. The reinforced EFPA consists of three parallel EFPAs with restraint PET plates, as depicted in **Fig. 3**. Each restraint plate, with a thickness of 1 mm, is inserted into each bellows of the sleeve in the EFPA, which keeps each actuator arranged 120° from each other at a radius of 11 mm from the center of the reinforced EFPA. By using restraint plates, the reinforced EFPA can maintain its bending stiffness.

3. Spiral Shaped Soft Holding Actuator with Circumferential Restrains

To construct a spiral-shaped reinforced EFPA, the reinforced interval of bellows in each EFPA is fine tuned. **Fig. 4** shows an overview of the spiral actuator. The spiral actuator consists of three parallel EFPAs arranged with restraint plates, as shown in **Fig. 3**. The original length of each EFPA depicted in the figure is approximately 0.5, 1, and 2 m, respectively. 100 PET plates with a thickness of 1 mm were used for the spiral-shaped reinforced EFPA. The mass of the actuator is approximately 500 g. EFPAs 1, 2, and 3, as shown in **Fig. 4**, are different from the others and are restrained every one, two, and four bellows, respectively. Using this method, EFPA 1 is placed inside the actuator. EFPA 2 is arranged in a twisted shape. EFPA 3 is arranged on the outer side of the actuator.

The operating principle of the spiral-shaped actuator is as follows. **Fig. 5(a)** shows the operation of the tested actuator using extended EFPA 1. When EFPA 1 is pressurized, both the diameter and longitudinal length of the spiral-shaped actuator increase. It was found that the number of rolls in the spiral was less than that in the initial state. This means that the difference in the length of EFPAs 1 and 3 is small when the inner-side EFPA 1 is extended. Therefore, the diameter of the spiral actuator increases in the circumferential direction. The spiral actuator can be fit to the human body by changing its diameter. In general, it is expected that the total length of the spiral actuator decreases when the diameter increases. However, it can be observed that the total length of the actuator in-

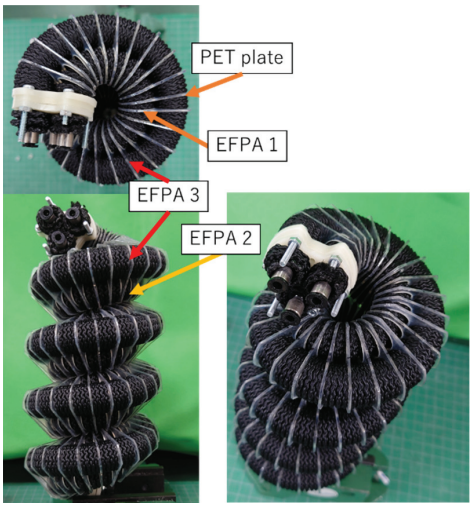

Fig. 4. Overview of spiral soft actuator with circumferential restrain mechanism.

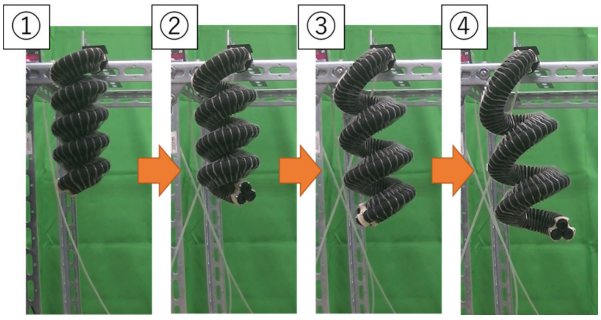

(a) Pressurization of EFPA 1 only

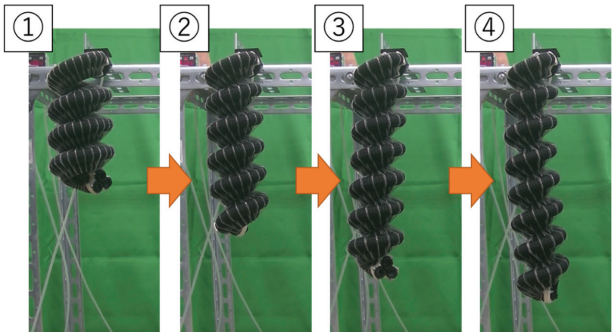

(b) Pressurization of EFPA 3 only

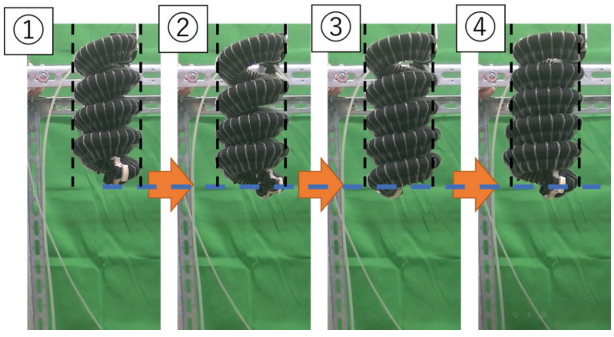

(c) Pressurization of all EFPAs

Fig. 5. Operation of spiral shaped actuator for various combinations of pressurized EFPAs.

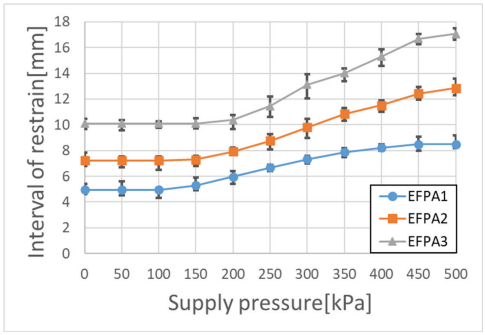

Fig. 6. Relation between supply pressure and interval of restraint each in EFPA.

creases in **Fig. 5(a)**. Note that the length increases owing to gravity as well. **Fig. 5(b)** shows the operation of the actuator using the extended EFPA 3. When EFPA 3 is pressurized, the diameter of the actuator decreases, and the longitudinal length of the actuator increases because only the outer side EFPA 3 is extended. It was found that the number of rolls in the actuator increased compared with that in the initial state. This means that EFPA 3 is extended only toward the inside of the actuator because the circumferential direction of the actuator is restrained by EFPA 1. **Fig. 5(c)** illustrates the operation of the actuator after pressurizing all EFPAs. When all EFPAs are pressurized, the diameter of the actuator increases. This means that the longitudinal length of the actuator is the same as the initial length because EFPAs 1–3 are extended by maintaining the same configuration. In **Fig. 5(c)**, it was observed that EFPA 1 is extended first, then EFPAs 2 and 3 are extended. This indicates that the motion is affected by the friction between the silicone rubber tube and bellows sleeve in the EFPA. The friction increases with an increase in the pitch of the restraint. The user can be wrapped and held by following the body and released by these motions.

Figure 6 shows the relation between the supply pressure and restraint interval for each EFPA. In **Fig. 6**, each symbol represents the restraint interval for each EFPA. In the experiment, the interval for each EFPA was measured when it was pressurized from 0 to 500 kPa at every 50 kPa. The interval for each supply pressure was measured ten times using a ruler. As a result, it can be observed that the maximum intervals of restrain in EFPAs 1, 2 and 3 are approximately 8.5, 12.9, and 17.1 mm, respectively, which are 1.7-, 1.8-, and 1.7-times extension of their initial intervals, respectively. Note that the minimum driving pressure for each EFPA is different. This is caused by friction, as mentioned above.

Figure 7 presents an overview of the experimental setup to measure the grasping force generated by the tested actuator. In the experiment, when EFPA 1 was pressurized, the tested actuator was inserted into a PVC pipe with an outer diameter of 76 mm. The midpoint of the actuator was connected to a force sensor with a wire. We define the wrapping force as the force required to remove the actuator from the wrapped object. When

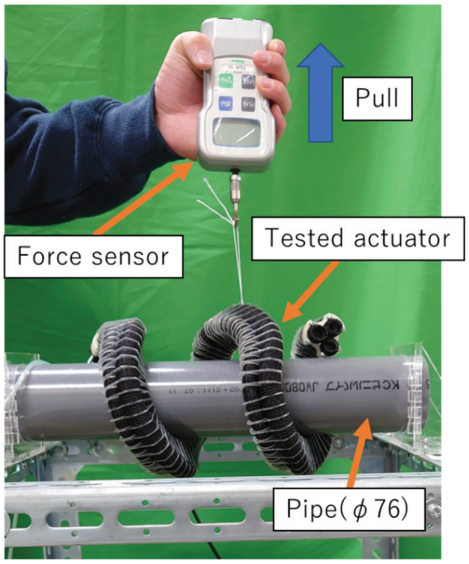

Fig. 7. Overview of the experimental setup used to measure the wrapping force of the actuator.

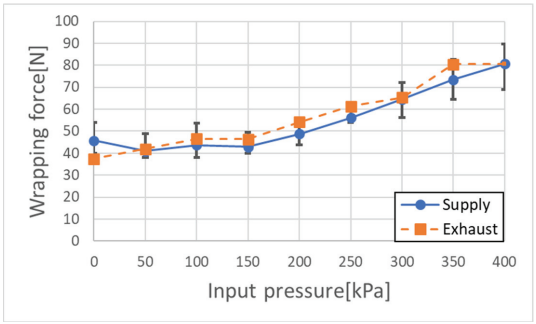

Fig. 8. Relationship between input pressure and wrapping force.

EFPA 3 was pressurized from 0 to 400 kPa, the wrapping force was measured five times using a force sensor (NIDEC-SHIMPO Corp., FGJN-50) at every 50 kPa. In addition, to investigate the hysteresis characteristics, when EFPA 3 was decompressed from 400 to 0 kPa, the force was measured once at every 50 kPa. **Fig. 8** illustrates the relationship between the input pressure and wrapping force of the actuator. In **Fig. 8**, the circles and squares denote the experimental results when pressure was supplied and exhausted, respectively. The vertical bar indicates the distribution of the measured data when the input pressure was increased. It was observed that the wrapping force of the tested actuator increased with the input pressure. The actuator buckled when the input pressure exceeded 450 kPa. We obtained a maximum wrapping force of approximately 80 N, despite a slippery PVC pipe was used. Therefore, the actuator can wrap a typical arm (approximately 3.6 kg) to lift it up [17].

In addition, to confirm the soft-wrapping performance, it is necessary to measure the wrapping pressure of the actuator when it wrapped around an object. **Fig. 9** shows an overview of the experimental setup used to measure the actuator wrapping pressure. During the experiment, the

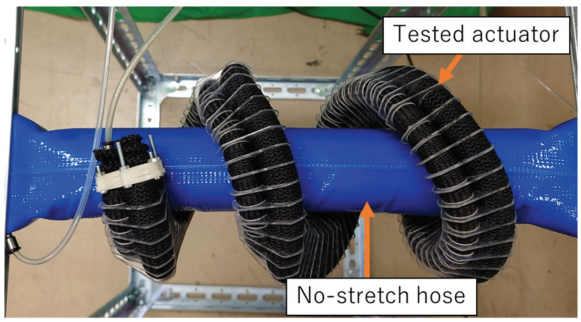

Fig. 9. Overview of the experimental setup used to measure the wrapping pressure of the actuator.

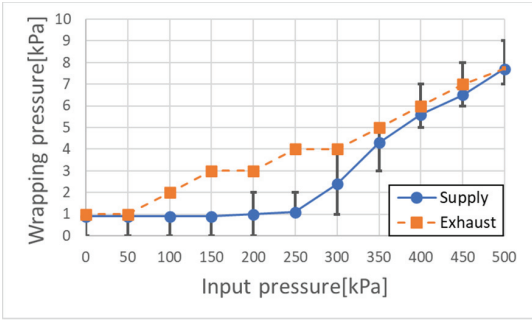

Fig. 10. Relationship between input and wrapping pressures.

actuator was inserted into an initial pressurized no-stretch hose (Kakuichi Co. Ltd., Maxflow SD φ50) at 3 kPa. We define the wrapping pressure as the inner pressure change in "no-stretch hose" wrapped by the tested actuator, as shown in **Fig. 9**. The wrapping pressure was measured 10 times using a pressure transducer (KEYENCE Corp., AP-C33) when the input pressure supplied to EFPA 3 in the actuator was varied. In addition, to investigate the hysteresis characteristics, when EFPA 3 was decompressed from 500 to 0 kPa, the wrapped pressure was measured once at every 50 kPa. **Fig. 10** shows the relationship between the input pressure supplied to EFPA 3 and wrapping pressure of the actuator. In **Fig. 10**, the circles and squares denote the experimental results when pressure was supplied and exhausted, respectively. The vertical bar indicates the distribution of the measured data when the input pressure was increased. As a result, we determined that a not-so-large wrapping pressure of 7.7 kPa (58 mmHg) could be obtained. Note that there was distinct hysteresis during the supply and exhaustion of pressures. It is caused by the hysteresis of the EFPA. In summary, the actuator has the advantage of being able to wrap an object softly with a relatively large wrapping force of approximately 80 N and low wrapping pressure of 7.7 kPa (58 mmHg). By using a longer spiral-shaped actuator, we can expect that the wrapping force increases with the same wrapping pressure.

In order to make sure that the held joint can bend even if the tested actuator wraps the joint, certain experiments were conducted. **Fig. 11** shows a transient view of moving while the actuator is holding the elbow of the test subject.

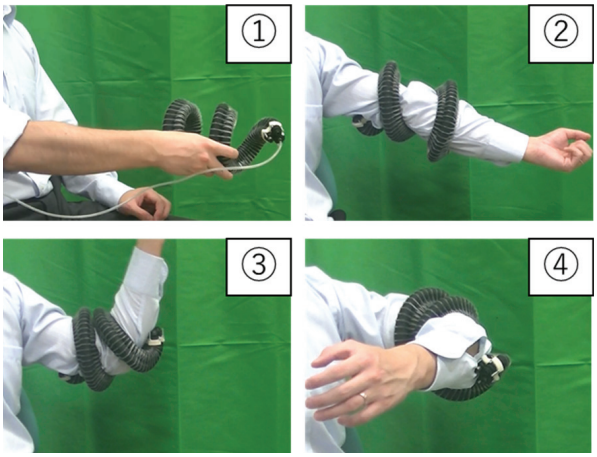

Fig. 11. Transient view of moving the joint while holding.

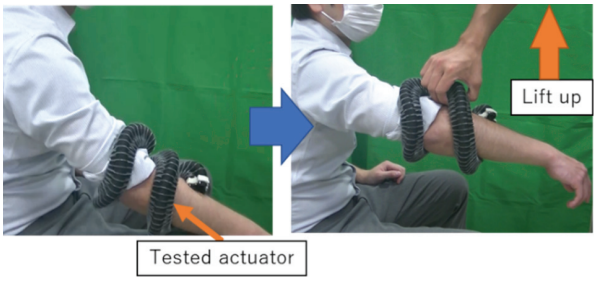

Fig. 12. Transient view of a lifted-up arm.

As shown in **Fig. 11**, an actuator with a larger diameter is worn on the user's joint. The joint can be wrapped by decompressing the pressurized actuator. Consequently, it was observed that the joint can bend even if the actuator holds the joint.

In order to make sure that the actuator could wrap and hold the body, the actuator holding the body was lifted. **Fig. 12** shows the transient view of a lifted-up arm while being held using the spiral actuator. In the experiment, when EFPA 1 was pressurized with a supply pressure of 500 kPa, the spiral-shaped actuator could be worn on the arm. The user's arm or knee was wrapped by decompressing the pressurized EFPA 1. Under these conditions, when EFPA 3 was pressurized with a supply pressure of 300 kPa, the actuator could hold surely as a result of a wrapping motion. In **Fig. 12**, it was observed that the actuator was wrapped onto to the user's arm without buckling. It was also confirmed that the actuator wrapped the arm and did not come off when the actuator was lifted.

As shown in **Fig. 13**, the actuator could be worn on the knee as well. Note that the actuator is not wrapped because the knee is thicker than the elbow. It can also be observed that the knee could be lifted, although the actuator was slightly extended. Therefore, the actuator had a holding force that could not be removed owing to the lifting maneuver. However, the actuator could not wrap around the joint owing to the joint size. An analytical model that can predict the diameter of a spiral actuator is required to design actuators according to the size of the joints.

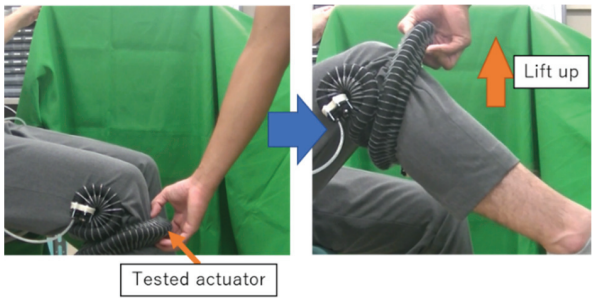

Fig. 13. Transient view of a lifted-up knee.

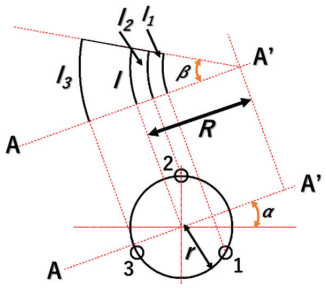

(a) Definition of restraint interval of each EFPA

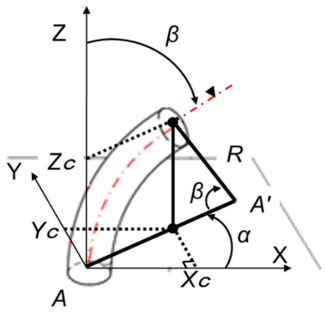

(b) Definition of angles α and β

Fig. 14. Analytical model of spiral shaped actuator within the restraint interval of each EFPA.

4. Analytical Model of Spiral Shaped Actuator with Circumference Restraint Mechanism

In order to design and predict the diameter of the spiral-shaped actuator according to the body shape in question, a static analytical model of the actuator is constructed. Particularly, it is necessary to calculate the diameter of the spiral-shaped actuator and length of each EFPA when one or two EFPAs are pressurized. To calculate the interval of restraint in each EFPA, an analytical model of the spiral-shaped actuator within the restraint of each EFPA, as shown in **Fig. 14**, is proposed [18].

In **Figs. 14(a)** and **(b)**, the interval of restraint in the spiral-shaped actuator located on the X-axis is defined as EFPA 1, and the other EFPAs that are arranged in a counterclockwise direction from the position of EFPA 1 are defined as EFPAs 2 and 3. l_1, l_2, and l_3 are the intervals of restraint in EFPAs 1, 2, and 3, respectively. From the geometric relationships shown in **Figs. 14(a)** and **(b)**, the

following equations can be obtained:

$$l_1 = (R - r\cdot\cos\alpha)\cdot\beta, \quad \ldots\ldots (1)$$

$$l_2 = \left\{R - r\cdot\cos\left(\frac{2\pi}{3}\alpha\right)\right\}\cdot\beta, \quad \ldots\ldots (2)$$

$$l_3 = \left\{R - r\cdot\cos\left(\frac{4\pi}{3} - \alpha\right)\right\}\cdot\beta, \quad \ldots\ldots (3)$$

$$R = \frac{l}{\beta}, \quad \ldots\ldots (4)$$

where l is the central interval of the restraint in the spiral actuator, R is the radius of curvature of the actuator, and r is the distance between the center of the actuator and center of each actuator. α and β are the bending directional and bending angles, respectively. Using Eqs. (1)–(4), the central interval of restraint in actuator l, bending directional angle α, and bending angle β can be stated as the following equations:

$$\alpha = \tan^{-1}\frac{\sqrt{3}(l_3 - l_2)}{l_3 + l_2 + 2l_1}, \quad \ldots\ldots (5)$$

$$\beta = \frac{l - l_1}{r\cdot\cos\alpha}, \quad \ldots\ldots (6)$$

$$l = \frac{l_1 + l_2 + l_3}{3}. \quad \ldots\ldots (7)$$

Using these equations, each restraint interval in the EFPAs can be calculated.

Next, to calculate the shape of the spiral-shaped actuator, its central coordinates can be expressed by the following equation:

$$\begin{pmatrix} x_c \\ y_c \\ z_c \end{pmatrix} = \begin{pmatrix} R\cdot(1-\cos\beta)\cdot\cos\alpha + x_e \\ R\cdot(1-\cos\beta)\cdot\sin\alpha + y_e \\ R\cdot\sin\beta + z_e \end{pmatrix}, \quad \ldots (8)$$

where x_c, y_c, and z_c are the central coordinates of the spiral actuator, respectively. x_e, y_e, and z_e are the extension factors in the axis direction to prevent interference from the actuator. Furthermore, to calculate the recent coordinate at every restraint interval, the coordinate that was calculated for each restraint interval of each EFPA is required. The recent coordinate for every restraint interval in actuator $\boldsymbol{P}_n$ is given by the following equation:

$$\boldsymbol{P}_n = \begin{pmatrix} x_n \\ y_n \\ z_n \\ 1 \end{pmatrix} = \boldsymbol{P}_c\cdot\boldsymbol{R}_z(\alpha)\cdot\boldsymbol{R}_y(\beta)\cdot\boldsymbol{P}_{n-1}, \quad \ldots (9)$$

$$\boldsymbol{P}_c = \begin{pmatrix} 1 & 0 & 0 & x_c \\ 0 & 1 & 0 & y_c \\ 0 & 0 & 1 & z_c \\ 0 & 0 & 0 & 1 \end{pmatrix}, \quad \ldots\ldots (10)$$

$$\boldsymbol{R}_z(\alpha) = \begin{pmatrix} \cos\alpha & -\sin\alpha & 0 & 0 \\ \sin\alpha & \cos\alpha & 0 & 0 \\ 0 & 0 & 1 & 0 \\ 0 & 0 & 0 & 1 \end{pmatrix}, \quad \ldots\ldots (11)$$

$$\boldsymbol{R}_y(\beta) = \begin{pmatrix} \cos\beta & 0 & \sin\beta & 0 \\ 0 & 1 & 0 & 0 \\ -\sin\beta & 0 & \cos\beta & 0 \\ 0 & 0 & 0 & 1 \end{pmatrix}, \quad \ldots\ldots (12)$$

where $\boldsymbol{P}_c$ is the translation of the restraint and $\boldsymbol{R}_z(\alpha)$ and $\boldsymbol{R}_y(\beta)$ are the roll and pitch of the restraint plates, respectively. n is the number of restraint plates. The bending directional angle α after the second restraint plate becomes zero because it is changed only in the first plate.

Based on the Eqs. (4)–(9), the spiral-shaped actuator was simulated using MATLAB. In addition, based on the experimental results regarding the displacement of the EFPA for the input pressure, the displacement of each EFPA with respect to pressure was determined. **Fig. 15** shows the operation of the actuator using pressurized EFPA 1 or 3. The lines represent EFPAs 1, 2, and 3, respectively. From **Fig. 15(a)**, it appears that the simulated spiral-shaped actuator agrees with the experimental results as shown in **Fig. 5(a)**. The number of rolls in the actuator was decreased by extending EFPA 1. **Fig. 15(b)** shows that the number of rolls in the simulated spiral-shaped actuator increases while contracting the diameter when EFPA 3 is pressurized. It is also apparent that the simulated actuator agrees with the experimental results as shown in **Fig. 5(b)**.

To compare the calculated and experimental results, the diameter of the spiral-shaped actuator was measured. **Fig. 16** presents an overview of the experimental setup used to measure the diameter of the actuator. In the experiment, the center diameter of the actuator with a fixed tip was measured at every 50 kPa when EFPA 1 or 3 was pressurized from 0 to 500 kPa. The center diameter of the actuator was measured five times at each supply pressure. In addition, to investigate the hysteresis characteristics, when EFPA 3 was decompressed from 500 to 0 kPa, the diameter was measured once at every 50 kPa.

Figure 17 depicts the relation between the supply pressure and center diameter of the actuator. In **Fig. 17**, the circles and triangles denote the experimental results when pressure was supplied and exhausted, respectively. In addition, squares denote the calculated results. The vertical bar indicates the distribution of the measured data when the input pressure was increased. From **Fig. 17(a)**, it was observed that the calculated results agree with the experimental results for the supply case. As shown in **Fig. 17(b)**, observe that the calculated results relatively agree with experimental results for the supply case. However, as the supply pressure increases, the difference between the calculated and experimental results becomes slightly larger. It seems that the difference is caused by the interference and friction between the restraint PET plates because the diameter becomes too small. In addition, it was observed that there is a different tendency in the experimental results for the exhaust case between EFPAs 1 and 3. This can be explained based on the hysteresis characteristics of the EFPA. Because EFPA 1 was set at the innermost side, as shown in **Fig. 4**, when EFPA 1 was pressurized and extended, the diameter of the actuator increased, as

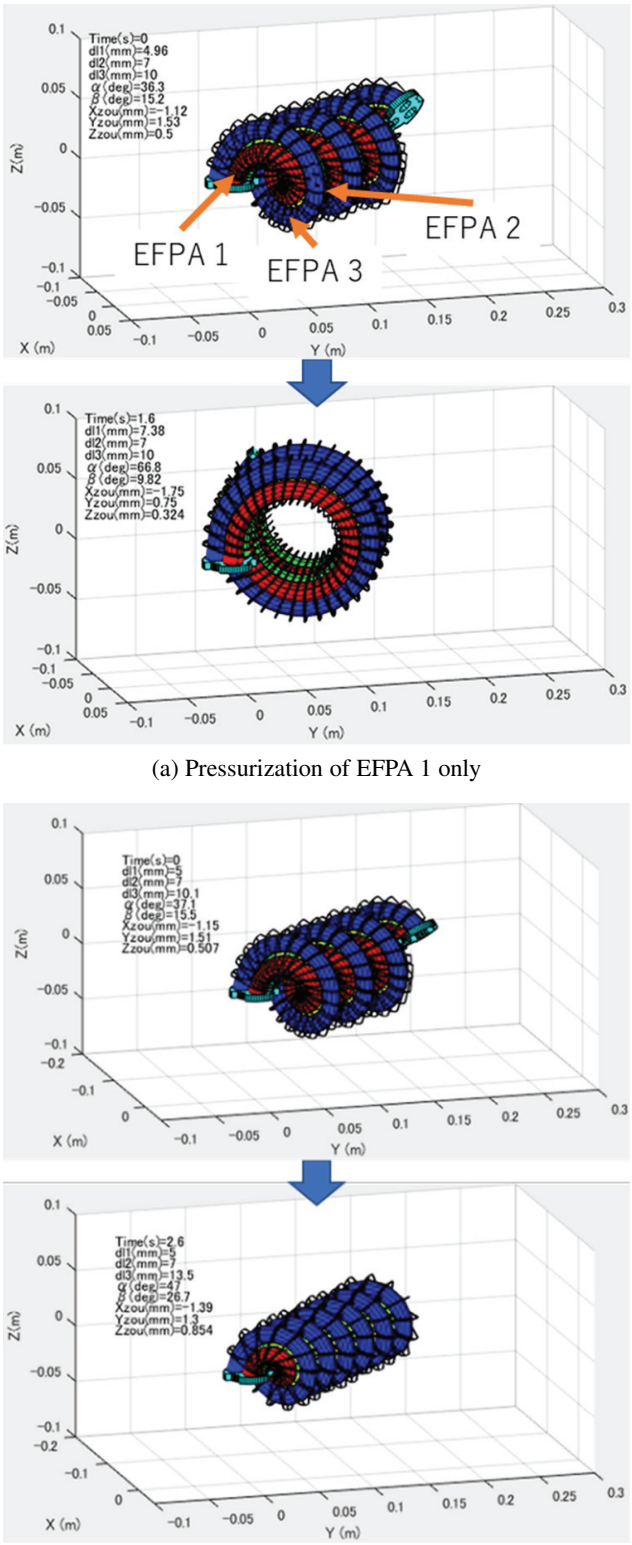

(a) Pressurization of EFPA 1 only

(b) Pressurization of EFPA 3 only

Fig. 15. Operation of calculated spiral actuator.

shown in **Fig. 17(a)**. When EFPA 1 was decompressed and contracted, its diameter decreased. However, owing to the hysteresis of the EFPA, the diameter of the actuator became larger than that for the same pressure. The hysteresis of the diameter presented in **Fig. 17(b)** can also be

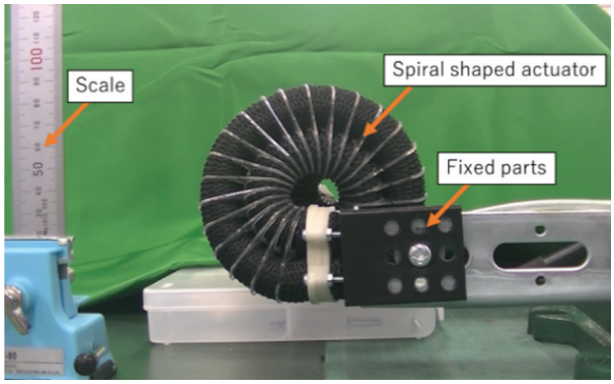

Fig. 16. Experimental setup used to measure the actuator diameter.

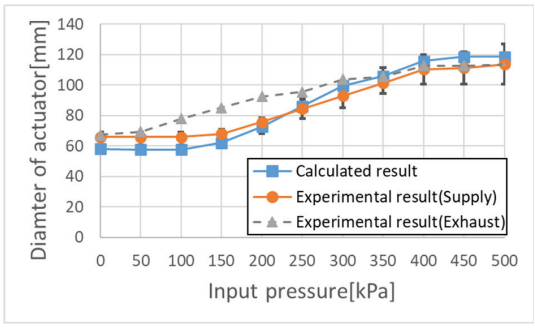

(a) Pressurization of EFPA 1 only

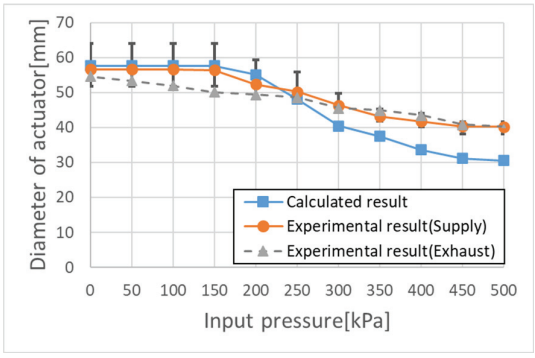

(b) Pressurization of EFPA 3 only

Fig. 17. Relation between supply pressure and diameter of the actuator.

explained in the same manner and by the fact that EFPA 3 is set at the outermost side, as shown in **Fig. 4**.

5. Conclusions

Because a soft holding actuator can wrap easily to hold a human body and release it, a spiral-shaped soft holding actuator using three EFPAs and a reinforced circumferential restraint mechanism was proposed and tested in this study. Consequently, it was confirmed that the tested actuator could wrap, hold, and release human joints according to the body shape by changing the pressurized EFPA. To investigate the holding ability of the tested actuator, the

knee and elbow joints were lifted using a wrapped actuator. It was found that the actuator could hold these joints when the wrapped joints could move freely. It was also confirmed that the body could be lifted-up while being held by the actuator.

In order to design and predict the diameter of the spiral-shaped actuator according to the body shape, a static analytical model of the tested actuator was proposed. It was found that the analytical model could be used to calculate the static behavior of the wrap and release motions achieved by changing the pressurized EFPA. In order to confirm the validity of the model, the calculated and experimental results for the actuator center diameter were compared. It was confirmed that the diameters generally agreed well. However, with an increase in the supply pressure for EFPA 3, the difference between the calculated and experimental results became slightly larger. The difference may have been caused by the interference and friction between restraint PET plates because the diameter of the actuator was too small.

In a future study, based on the proposed model, a spiral-shaped actuator with a suitable diameter will be developed to fit various parts of the human body. In addition, it is necessary to estimate the force distribution of the wrapping force and the pressure of the actuator to realize a safer wrapping device. Therefore, a model for the wrapping force considering the elasticity and relationship between the pressure and displacement of the EFPA is required. In addition, we will construct a dynamic model of the spiral-shaped actuator to control the wrapping motion according to the body shape.

References:

[1] Y. Nagata, "Soft Actuators, Forefront of Development," pp. 291-335, NTS Ltd., 2004.

[2] T. Noritsugu, M. Takaiwa, and D. Sasaki, "Development of Power Assist Wear Using Pneumatic Rubber Artificial Muscles," J. Robot. Mechatron., Vol.21, No.5, pp. 607-613, 2009.

[3] Y. Matsui, T. Akagi, S. Dohta, W. Kobayashi, and H. Tamaki, "Development of Flexible Spherical Actuator with 3D Coordinate Measuring Device," J. of Flow Control, Measurement & Visualization, Vol.6, No.2, pp. 95-106, 2018.

[4] C. Thakur, K. Ogawa, and Y. Kurita, "Active Passive Nature of Assistive Wearable Gait Augment Suit for Enhanced Mobility," J. Robot. Mechatron., Vol.30, No.5, pp. 717-728, 2018.

[5] C. Ishii and K. Yoshida, "Improvement of a Lightweight Power Assist Suit for Nursing Care," Int. J. of Engineering and Technology, Vol.11, No.4, pp. 256-261, 2019.

[6] T. Chang, S. Koizumi, H. Nabae, G. Endo, K. Suzumori, K. Hatakeyama, S. Chida, and Y. Shimada, "A Wearable Ankle Exercise Device for Deep Vein Thrombosis Prevention Using Thin McKibben Muscles," 2020 8th IEEE RAS/EMBS Int. Conf. for Biomedical Robotics and Biomechatronics (BioRob), pp. 42-47, 2020.

[7] N. Saito, D. Furukawa, T. Satoh, and N. Saga, "Development of Semi-Crouching Assistive Device Using Pneumatic Artificial Muscle," J. Robot. Mechatron., Vol.32, No.5, pp. 885-893, 2020.

[8] S. Kimura, R. Suzuki, K. Machida, M. Kashima, M. Okui, R. Nishihama, and T. Nakamura, "Development of an Exoskeleton-Type Assist Suit Utilizing Variable Stiffness Control Devices Based on Human Joint Characteristics," MDPI J. Actuators, Vol.10, No.1, 2021.

[9] J. Yan, X. Zhang, B. Xu, and J. Zhao, "A New Spiral-Type Inflatable Pure Torsional Soft Actuator," Soft Robotics, Vol.5, No.5, pp. 527-540, 2018.

[10] E. R. Perez-Guagnelli, S. Nejus, J. Yu, S. Miyashita, Y. Liu, and D. D. Damia, "Axially and Radially Expandable Modular Spiral Soft Actuator for Actuatoric Implantables," 2018 IEEE Int. Conf. on Robotics and Automation (ICRA), pp. 4297-4304, 2018.

[11] T. Mitsuda and Y. Kojima, "Spiral air gripper that coils around objects of various shapes," Proc. of the 2020 JSME Conf. on Robotics and Mechatronics, 1A1-J21, 2020.

[12] P. Yuan, G. Kawano, and H. Tsukagoshi, "Design and Modeling of Soft Pneumatic Spiral Actuator with High Contraction Ratio," J. Robot. Mechatron., Vol.32, No.5, pp. 1061-1070, 2020.

[13] S. Shimooka, T. Akagi, S. Dohta, W. Kobayashi, and T. Shinohara, "Improvement of Home Portable Rehabilitation Device For Upper-Limbs," JFPS Int. J. of Fluid Power System, Vol.12, No.1, pp. 10-18, 2019.

[14] W.-H. Tian, C.-C. Jhan, M. Inokuma, T. Akagi, S. Dohta, and S. Shimooka, "Development of Tetrahedral-Shaped Soft Actuator Arm as a Wrist Rehabilitation Device Using Extension Type Flexible Pneumatic Actuators," J. Robot. Mechatron., Vol.32, No.5, pp. 931-938, 2020.

[15] S. Shimooka, T. Akagi, S. Dohta, T. Shinohara, Y. Hane, and M. Aliff, "Development of Reinforced Extension Type Flexible Pneumatic Actuator with Circumferential Restraints and its Application for Rehabilitation Device," Int. J. of Automotive and Mechanical Engineering, Vol.17, No.3, pp. 8116-8127, 2020.

[16] S. Shimooka, Y. Hane, T. Akagi, S. Dohta, W. Kobayashi, T. Shinohara, and Y. Matsui, "Development and Attitude Control of Washable Portable Rehabilitation Device for Wrist Without Position Sensor," JFPS Int. J. of Fluid Power System, Vol.13, No.3, pp. 25-34, 2020.

[17] K. Ogawa, "Evidence-Based Nursing Ergonomics and Body-Mechanics," p. 28, Tokyo Denki University Press, 2008.

[18] M. Aliff, S. Dohta, and T. Akagi, "Trajectory Control of Actuator Arm Using Flexible Pneumatic Cylinders and Embedded Controller," Proc. of 2015 IEEE/ASME Int. Conf. on Advanced Intelligent Mechatronics, pp. 1120-1125, 2015.

Supporting Online Materials:

[a] Annual Report on the Ageing Society [Summary] FY 2019. https://www8.cao.go.jp/kourei/english/annualreport/2019/pdf/2019.pdf [Accessed August 18, 2021]

[b] The National Health and Nutrition Survey in Japan, 2019. https://www.mhlw.go.jp/content/000710991.pdf [Accessed February 21, 2022]

Name:
So Shimooka

Affiliation:
Assistant Professor, Graduate School of Natural Science and Technology, Okayama University

Address:
3-1-1 Tsushima-naka, Kita-ku, Okayama 700-8530, Japan

Brief Biographical History:
2020 Received Ph.D. degree from Okayama University of Science
2020-2021 Assistant Professor, National Institute of Technology, Matsue College
2021- Assistant Professor, Okayama University

Main Works:
• "Development of Reinforced Extension Type Flexible Pneumatic Actuator with Circumferential Restraints and its Application for Rehabilitation Device," Int. J. of Automotive and Mechanical Engineering, Vol.17, No.3, pp. 8116-8127, 2020.
• "Development and Attitude Control of Washable Portable Rehabilitation Device for Wrist Without Position Sensor," JFPS Int. J. of Fluid Power System, Vol.13, No.3, pp. 25-34, 2020.

Membership in Academic Societies:
• The Japan Fluid Power System Society (JFPS)
• The Japan Society of Mechanical Engineers (JSME)

Name:
Tetsuya Akagi

Affiliation:
Professor, Department of Intelligent Mechanical Engineering, Okayama University of Science

Address:
1-1 Ridai-cho, Kita-ku, Okayama 700-0005, Japan

Brief Biographical History:
1998- Research Associate, Tsuyama National College of Technology
2005- Lecturer, Okayama University of Science
2013- Professor, Okayama University of Science

Main Works:
• "Study of Wearable Pneumatic Control Device," 2010 Young Scientists' Prize from Ministry of Education, Culture, Sports, Science and Techno-logy (MEXT) in Japan.

Membership in Academic Societies:
• The Japan Society of Mechanical Engineers (JSME)
• The Society of Instrument and Control Engineers (SICE)
• The Robotics Society of Japan (RSJ)
• The Japan Fluid Power System Society (JFPS)

Name:
Shujiro Dohta

Affiliation:
Professor Emeritus, Department of Intelligent Mechanical Engineering, Okayama University of Science

Address:
1-1 Ridai-cho, Kita-ku, Okayama 700-0005, Japan

Brief Biographical History:
1974- Research Associate, Okayama University of Science
1984-1985 Exchange Faculty of Wright State University
1993- Professor, Okayama University of Science
2015-2018 Vice President, Okayama University of Science

Main Works:
• "Development of a Tetrahedral-Shaped Soft Robot Arm as a Wrist Rehabilitation Device Using Extension Type Flexible Pneumatic Actuators," J. Robot. Mechatron., Vol.32, No.5, pp. 931-938, 2020.
• "Development of Low-Cost Pressure Control Type Valves Using Buckled Tubes and Gate-mechanism," JFPS Int. J. of Fluid Power System, Vol.14, No.1, pp. 28-34, 2021.

Membership in Academic Societies:
• The Japan Fluid Power System Society (JFPS)
• The Japan Society of Mechanical Engineers (JSME)

Name:
Takashi Shinohara

Affiliation:
Design and Manufacturing Center, Organization for Research Development and Outreach, Okayama University of Science

Address:
1-1 Ridai-cho, Kita-ku, Okayama 700-0005, Japan

Brief Biographical History:
2007 Received Doctor of Engineering from Graduate School of Engineering, Okayama University of Science
2008- Teacher, Mechanics Department, Okayama University of Science High School
2017- Educational Lecturer, Learning Support Section, Center for Fundamental Education, Institute for the Advancement of Higher Education, Okayama University of Science
2021- Technical Educational Lecturer, Design and Manufacturing Center, Organization for Research Development and Outreach, Okayama University of Science

Main Works:
• "Analysis and Improvement of Cilia Type Pipe Inspection Robot Using Extension Type Flexible Pneumatic Actuators," JFPS Int. J. of Fluid Power System, Vol.14, No1, pp. 19-27, 2021.

Membership in Academic Societies:
• The Japan Fluid Power System Society (JFPS)

Name:
Takumi Kobayashi

Affiliation:
Department of System Science, Doctoral Program of Engineering, Okayama University of Science

Address:
1-1 Ridai-cho, Kita-ku, Okayama 700-0005, Japan

Brief Biographical History:
2022 Graduated from Graduate Program of Engineering, Okayama University of Science
2022- Doctoral Program of Engineering, Okayama University of Science
2022- JSPS Research Fellowship for Young Scientists (DC)

Main Works:
• T. Kobayashi et al., "Development of Small-Sized Servo Valve Using Gate Mechanism and Diaphragm," JFPS Int. J. Fluid Power System, Vol.14, No.1, pp. 1-9, 2021.
• T. Kobayashi et al., "Development of low-cost pressure control type valves using buckled tubes and gate-mechanism," JFPS Int. J. Fluid Power System, Vol.14, No.1, pp. 28-34, 2021.
• T. Kobayashi et al., "Development of Tetrahedral-type Soft Actuators Driven by Low-Cost Servo Valves Using RC Servo Motors," JFPS Int. J. Fluid Power System, Vol.14, No.2, pp. 35-42, 2021.

Membership in Academic Societies:
• The Japan Fluid Power System Society (JFPS)